Journal of Andrology, Vol. 18, No. 3, May/June 1997

Effects of Heat Stress on Mouse Testicular Cells and Sperm Chromatin Structure

BRIAN L. SAILER, LINDA J. SARKAR, JANET A. BJORDAHL, LORNA K. JOST, AND DONALD P. EVENSON

From the South Dakota State University, Department of Chemistry and Biochemistry, Olson Biochemistry Laboratories, Brookings, South Dakota.

ABSTRACT: Scrotal regions of mice were exposed to a 38.0, 40.0, or 42.0°C (±0.1) H_2O bath for 60 minutes to determine the effects of elevated temperatures on testicular cells and sperm chromatin structure. Mice were killed on various days after exposure, and ratios of acridine orange-stained testicular cell populations were determined by flow cytometry. Testicular weights of mice exposed to 42.0°C decreased significantly day 1 ($P < 0.01$) through 35 ($P < 0.001$). Also, a significant relative decrease in testicular haploid cells was seen on days 3–35 ($P < 0.001$) with a corresponding increase in the diploid population ($P < 0.001$). Testicular analyses of mice exposed to 38.0°C were not significantly different from control values. Testis weights of mice exposed to 40.0°C were not affected, but a relative decrease in percent haploid cells occurred on days 11 and 14 ($P < 0.001$). The sperm chromatin structure assay (SCSA) was used to measure the susceptibility of cauda epididymal sperm DNA to *in situ* denaturation at low pH. Caudal epididymides of mice exposed to 42.0°C had no sperm. Caudal epididymal sperm from mice exposed to 40.0°C were most susceptible to acid-induced DNA denaturation on days 3 ($P < 0.05$), 7, 11, and 14 (all $P < 0.001$). The 38.0°C exposed mice showed some minor sperm chromatin abnormalities at later time points (days 11–35). When compared to sperm head morphology measurements, SCSA parameters were more sensitive indicators of heat-induced sperm abnormalities. These results show that mouse spermatogenesis is disrupted by scrotal exposure to environmental temperatures several degrees over normal physiological temperature and, of more biological interest, that some thermal ranges above normal allowed production of sperm with compromised nuclear chromatin structure.

Key words: Testicular heat stress, SCSA.
J Androl 1997;18:294–301

Sensitivity of mammalian germ cells to environmental heat has been well documented (Ulberg, 1958) with the effects of hyperthermia being recorded for a variety of species including mice (Meistrich et al, 1973b), rats (Chowdhury and Steinberger, 1964), bulls (Casady et al, 1953; Vogler et al, 1991), rams (Mieusset et al, 1991), and humans (Levine et al, 1990). Studies on rodents have included experiments based on histological observations (Collins and Lacey, 1969), testicular weight (Hand et al, 1979), testicular kinetics (Meistrich et al, 1973a), and determination of testicular-cell populations monitored by flow cytometric (FCM) measurement of cellular DNA stainability (De Vita et al, 1987).

Protein denaturation is the primary thermal-inactivation process occurring during hyperthermia in contrast to alterations in DNA synthesis that occur following ionizing radiation (Westra and Dewey, 1971). Spermatogenesis is a complex series of mitotic and meiotic cell divisions and dramatic cell differentiation culminating in the production of mature sperm cells (Russell et al, 1990). During spermiogenesis, the last phase of spermatogenesis, nuclear histones are replaced by testis-specific variants, followed by sperm-specific transition proteins, and eventually by protamine molecules (Meistrich et al, 1978). Spermatocytes are the testicular population that appears to be most sensitive to mild hyperthermia (Collins and Lacy, 1969; Oakberg, 1955), but the processes involved in spermiogenesis may also be adversely affected.

Acridine orange (AO) has been used in conjunction with FCM measurements to monitor the effects of toxic insults on mouse testicular cells and cauda epididymal sperm (Evenson et al, 1986a, 1993; Evenson and Jost, 1993; Sailer et al, 1995). Acridine orange intercalated into double-stranded DNA (dsDNA) fluoresces green, while AO bound to single-stranded RNA or single-stranded DNA (ssDNA) fluoresces red. By utilizing the metachromatic properties of AO (Darzynkiewicz, 1979), eight testicular-cell populations can be resolved and monitored (Evenson and Melamed, 1983; Evenson et al, 1986a). The sperm chromatin structure assay (SCSA) uses AO to monitor the susceptibility of sperm chromatin DNA to acid-induced denaturation *in situ* (Darzynkiewicz et al,

Supported in part by U.S. Environmental Protection Agency grant R820968-01. This is South Dakota State University Agricultural Experiment Station Publication No. 2965 of the journal series.

Correspondence to: Dr. Donald P. Evenson, Olson Biochemistry Laboratories, South Dakota State University, Box 2170, ASC 136, Brookings, South Dakota 57007.

Received for publication October 25, 1996; accepted for publication January 21, 1997.

1976; Evenson et al, 1980, 1985; Evenson and Jost, 1994).

Prior experiments have shown the SCSA to be a sensitive measure of sperm chromatin structure as related to fertility (Ballachey et al, 1987; Evenson et al, 1991) and reproductive toxicology. Exposure of mice by i.p. injection to triethylenemelamine (Evenson et al, 1989), thiotepa (Evenson et al, 1986a), ethylnitrosourea (Evenson et al, 1985), and hydroxyurea (Evenson and Jost, 1993) caused alterations in the relative ratios of testicular-cell populations indicative of damage to precursor spermatogonial stem cells and/or spermatogonia. Exposure to methyl methanesulfonate (Evenson et al, 1993) caused chromatin damage in elongated spermatids as well as in epididymal sperm due to alkylation of protamine sulfhydryl groups and subsequent DNA damage resulting in dominant lethal mutations (Sega and Owens, 1983).

In the current study, we have utilized AO staining in conjunction with FCM measurements to determine the testicular populations most sensitive to hyperthermia and to evaluate the utility of the SCSA for measuring thermal effects on sperm chromatin structure. Temperatures in the range of environmental to pathological (38.0–42.0°C) were investigated at different time points after mouse scrotal exposure to heat. Sperm head morphology analysis (Wyrobek and Bruce, 1975) was used as a comparative biomarker.

Materials and Methods

Mice

Five-to-six-week-old male B6C3F1/J mice (C57BL/6J × C3H/HeJ) obtained from the Jackson Laboratory (Bar Harbor, Maine) were acclimatized at our facility for 10 weeks prior to heat exposure. Animals were housed in transparent polycarbonate cages with stainless steel lids and pine shavings for bedding. Mice were allowed access to Purina Certified Rodent Chow and deionized water *ad libitum*. Caged mice were kept in a 21 ± 2°C room on a 12 hour light/dark schedule.

Hyperthermic Exposure and Cell Isolation

Mice were anesthetized with 100 mg/kg sodium pentobarbital (Nembutal) and placed into custom-made styrofoam rafts with holes for the scrotal region to protrude from the bottom. The rafts were floated in a thermostatically controlled water bath. A fan moved ambient air across the water surface to keep the unsubmerged portion of the animals cool. Testes were exposed to 38.0°C, 40.0°C, or 42.0°C (all ± 0.1) for 60 minutes. Control mice were anesthetized without exposure to elevated temperatures. Three mice were thermally exposed for each time point studied for each temperature level. The 38.0°C (n = 18) and 40.0°C (n = 15) thermally stressed mice shared the same controls (n = 9). The 42.0°C (n = 21) thermally exposed mice were evaluated with different control mice (n = 14).

At various time points following heat stress (38.0°C: 3, 7, 11, 14, 28, and 35 days; 40.0°C: 3, 7, 11, 14, and 35 days; 42.0°C: 1, 3, 7, 14, 21, 28, and 35 days), mice were anesthetized, killed by cervical dislocation, and weighed. The testes and cauda epididymides were surgically removed and testicular weights recorded. All tissues were kept on crushed ice (4°C) from the time of dissection until FCM measurement of fresh testicular samples or freezing (−100°C) of epididymal samples for later analysis.

Testes or cauda epididymides were placed in 60 mm petri dishes containing 1–2 ml Hanks' balanced salt solution (HBSS, Gibco, Grand Island, New York) or TNE buffer (0.01 M Tris-HCl, 0.15 M NaCl, 0.001 M disodium EDTA, pH 7.4), respectively. The tissues were minced with curved surgical scissors to liberate individual cells. Cell suspensions were pipetted into 12 × 75 mm conical tubes and the tissue fragments allowed to settle for several minutes. The supernatant was gravity filtered through 53 μm (testis) or 153 μm (epididymides) Nitex filters (Tetko Inc., New York, New York). Testicular samples were analyzed immediately, while filtered epididymal cell suspensions were split into two aliquots and were frozen (−100°C) for later analysis. A single freezing and thawing of epididymal sperm has no detrimental effect on SCSA data (Evenson et al, 1989, 1993, 1994).

Cell Staining With Acridine Orange

Two hundred microliter aliquots of fresh testicular- or thawed (37°C) epididymal-sperm cell suspensions (1–2 × 10^6/ml) were admixed with 0.40 ml of 0.1% Triton X-100, 0.15 M NaCl, and 0.08 N HCl, pH 1.2. Thirty seconds later, cells were stained by adding 1.2 ml of staining solution containing 6 μg chromatographically purified AO (Polysciences Inc., Warrington, Pennsylvania) per ml of AO buffer (370 ml of stock 0.1 M citric acid, 630 ml of stock 0.2 M Na_2HPO_4, 1 mM disodium EDTA, 0.15 M NaCl, pH 6.0) (Darzynkiewicz et al, 1975; Evenson and Jost, 1994). Triton X-100 was used in the first step of this procedure to permeabilize cell membranes, thereby, providing accessibility of DNA for AO staining. When excited by blue laser light (488 nm) the fluorescence from AO-stained testicular cells reflects the relative DNA (green fluorescence) vs. RNA (red fluorescence) content (Darzynkiewicz, 1979; Evenson and Melamed, 1983; Evenson et al, 1986b).

Sperm Chromatin Structure Assay

Acridine orange staining and subsequent FCM measurement of epididymal, vas deferens, or ejaculated sperm has been termed the sperm chromatin structure assay (SCSA; Evenson, 1989, 1990; Evenson and Jost, 1994). Even though the low pH treatment does not cause denaturation of histone-complexed DNA, it apparently does cause partial denaturation of protamine-complexed DNA in sperm having abnormal chromatin structure (Evenson et al, 1985). Abnormal chromatin structure, defined here as an increased susceptibility to acid induced denaturation *in situ*, is quantitated by FCM measurement of the shift from green (native, dsDNA) to red (denatured, ssDNA) fluorescence. The extent of this shift is expressed by alpha t (α_t) (Darzynkiewicz et al, 1975) and is the ratio of red to (red + green) fluorescence. Since normal mature epididymal-sperm cells contain virtually no RNA (Monesi, 1965), red fluorescence is minimal (Ev-

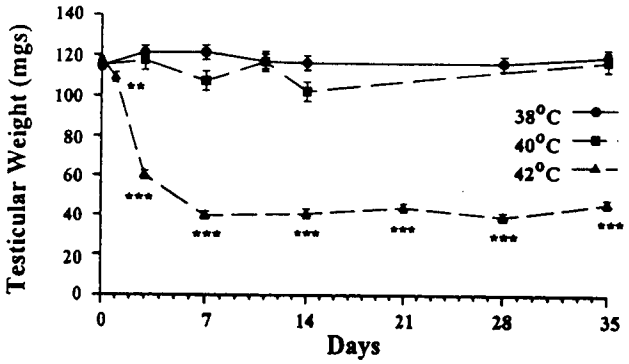

FIG. 1. Effects of scrotal heat on mouse testicular weights (least squares means [LSMeans] ± standard error of the mean [SEM]) as a function of time following exposure. Control values are plotted as day 0. Scrotal regions were exposed to 38.0°C, 40.0°C, or 42.0°C (all ±0.1) for 60 minutes. Control mice were anesthetized without exposure to elevated temperatures. Three mice were thermally exposed for each time point studied for each temperature level. The 38.0°C (n = 18; days 3, 7, 11, 14, 28, and 35) and 40.0°C (n = 15; days 3, 7, 11, 14, and 35) thermally stressed mice shared the same controls (n = 9). The 42.0°C (n = 21; days 1, 3, 7, 14, 21, 28, and 35) thermally exposed mice were evaluated with different control mice (n = 14). Body and testis weights did not differ between the two control groups. ** = $P < 0.01$; *** = $P < 0.001$.

enson and Melamed, 1983). Normal whole sperm cells treated with RNAse or sonicated and purified sperm nuclei demonstrate the same fluorescent pattern as untreated whole sperm cells, indicating red fluorescence is due to ssDNA staining and not nuclear or cytoplasmic RNA (Evenson et al, 1985; Ballachey et al, 1987).

Alpha t is calculated for each sperm cell in a sample and results are expressed as the mean ($X\alpha_t$), standard deviation ($SD\alpha_t$), and percentage of cells outside the main population of α_t ($COMP\alpha_t$) for each sample. Measurement of normal sperm produces a narrow α_t distribution. A sperm population with denatured, ssDNA has a broader α_t distribution hence larger $X\alpha_t$, $SD\alpha_t$, and $COMP\alpha_t$ values.

Flow Cytometry

Immediately after staining, cells were passed through the quartz flow channel of a Cytofluorograf 30 interfaced to a 2150 Data Handler (Ortho Diagnostics Inc., Westwood, Massachusetts). The flow cytometer had ultrasense optics and a Lexel 100 mW argon ion laser operated at 35 mW with an excitation wavelength of 488 nm. Recorded measurements were begun 3 minutes after staining, which allowed time for equilibration of the sample within the sheath flow. Data were collected on 5,000 cells per sample at a flow rate of ≈200 cells per second. Red ($F_{\geq 630}$) and green fluorescence ($F_{515-530}$) emitted from individual cells were separated optically and the digitized signals, processed in area mode (testicular cells) or peak mode (caudal sperm), were stored as list mode files on a computer diskette.

Data Analysis

Testicular-list mode files were analyzed using the 2150 Data Handler. Cauda epididymal-list mode files were converted to histogram files by the 2150 Data Handler and transferred via Multlink (Phoenix Flow Systems, San Diego, California) to an IBM PC compatible computer and analyzed using Multi2D software (Phoenix Flow Systems). Data were statistically analyzed using the General Linear Model (GLM) procedure of the Statistical Analysis System (SAS for Windows, 1996). Results were graphed using Sigma Plot for Windows software.

Sperm Morphology Analysis

Filtrate containing cauda epididymal sperm was mixed 1:1 with filtered 1% Eosin Y (H_2O) for 30 minutes and smeared on microscope slides. Two slides per sperm sample were made and allowed to air-dry overnight. Excess Eosin Y was removed by

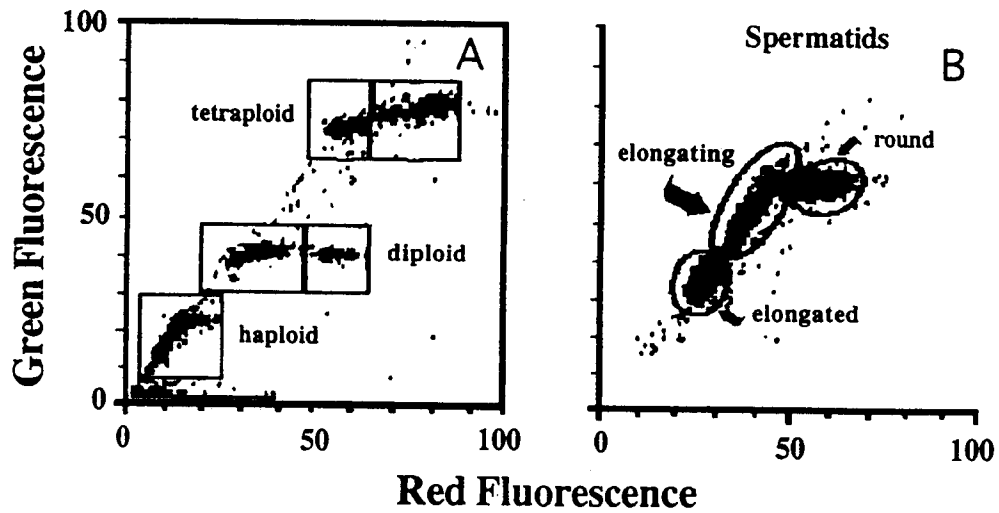

FIG. 2. Red- (RNA) vs. green- (DNA) fluorescence cytograms of acridine orange-stained testicular cells from a control mouse. **Panel A** shows three major discernible populations: i.e., tetraploid, diploid, and haploid cells. Two subpopulations are resolved in the tetraploid and diploid populations. S-phase cells are located between the tetraploid and diploid populations. **Panel B** is a computer magnification of the haploid population from panel A, resolving round, elongating, and elongated spermatids. The relative percentage of each cell type present was calculated from the number of cells in each gated population.

dipping slides briefly in methanol and again drying overnight. Coverslips were applied using Permount (Fisher Scientific, Fairtown, New Jersey) before microscopic examination. A Nikon Optiphot light microscope with differential interference contrast optics (100 × oil immersion) was used for the morphologic examination of sperm heads. The percent abnormal sperm heads was calculated from counting three samples per time point for a total of 1 × 10^3 sperm heads/sample (Wyrobek and Bruce, 1975).

Results

Controls

Control values are given as day 0 values in the plotted figures. No testicular parameter (percentage haploid, diploid, and tetraploid cells and percentage round, elongating, and elongated spermatids) differed significantly across the days of the experiment within the control group for 38.0°C and 40.0°C exposure or the control group for 42.0°C exposure; they also did not differ between the two control groups. Body and testis weights did not differ between the control group for 38.0°C and 40.0°C exposure and the control group for 42.0°C exposure. For the heat-stressed mice, each day was tested against the corresponding control group.

Body Weights

There were no significant changes in body weight for mice exposed to 38.0°C or 40.0°C, while mice exposed to 42.0°C were significantly different from controls (mean = 34.4 g) on days 3 (26.8 g; 22%, $P < 0.001$), 7 (29.8 g; 13%, $P < 0.01$), and 35 (37.8 g; 10%, $P < 0.05$). There was a definite loss of weight between days 1 and 3 through day 7 with recovery almost completed by day 14 (32.9 g; 5%, $P = 0.12$).

Testicular Weights

Testis weights of mice exposed to 38.0°C or 40.0°C were not different from control values over the duration of the experiment (Fig. 1). The 42.0°C exposed mice had dramatic testis weight losses during the entire experiment (day 1, $P < 0.01$; days 3–35, $P < 0.001$).

Testicular Cells

Flow cytometry data consisting of two-parameter red- (RNA) vs. green- (dsDNA) fluorescent cytograms of AO-stained testicular cells were obtained for all control and thermally stressed mice to assess changes in the ratios of testicular-cell types. An example of data from a control mouse is shown in Figure 2A; the eight discernible populations represent two tetraploid, two diploid, three haploid, and S-phase populations. Figure 2B is a computer enhancement for the resolution of the haploid subpopulations (round, elongating, and elongated spermatids).

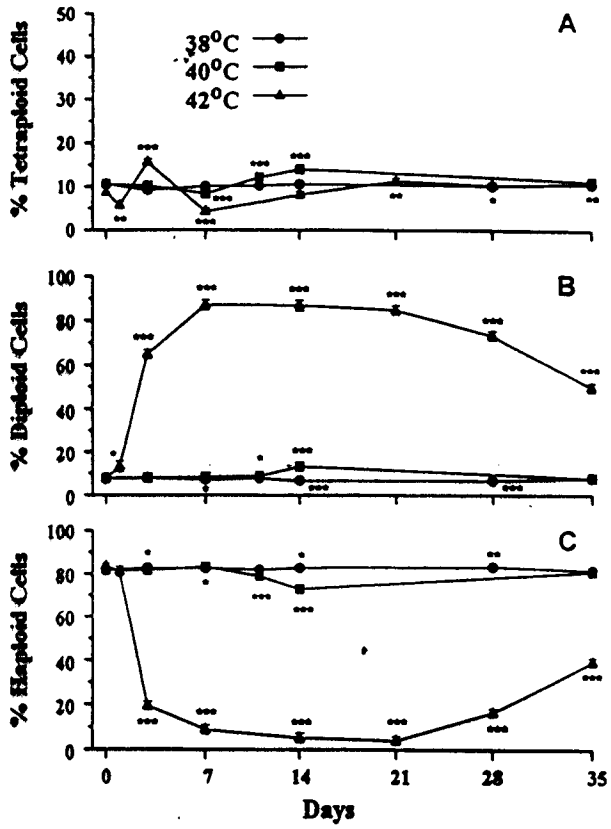

FIG. 3. Effects of scrotal heat on the major populations of acridine orange-stained mouse testicular cells plotted over time following thermal exposure. The values were determined from computer analysis of flow cytometric cytograms similar to that shown in Figure 2A. LSMeans ± SEM were plotted for tetraploid (A), diploid (B), and haploid (C) testicular populations. Scrotal regions were exposed to 38.0°C, 40.0°C, or 42.0°C (all ± 0.1) for 60 minutes. Control mice were anesthetized without exposure to elevated temperatures and are plotted as day 0. Three mice were thermally exposed for each time point studied for each temperature level. The 38.0°C (n = 18; days 3, 7, 11, 14, 28, and 35) and 40.0°C (n = 15; days 3, 7, 11, 14, and 35) thermally stressed mice shared the same controls (n = 9). The 42.0°C (n = 21; days 1, 3, 7, 14, 21, 28, and 35) thermally exposed mice were evaluated with different control mice (n = 14). Percentage haploid, diploid, and tetraploid cells did not differ between the control group for 38.0°C and 40.0°C exposure and the control group for 42.0°C exposure. * = $P < 0.05$; ** = $P < 0.01$; *** = $P < 0.001$.

The relative percentages of the testicular-cell populations present over time after thermal stress was temperature dependent (Fig. 3). Mice exposed to 38.0°C had only slight differences from controls in the relative percent of haploid ($P < 0.05$) and diploid ($P < 0.01$) populations. All three testicular populations varied significantly ($P < 0.001$) from control at 11 and 14 days when scrotal areas were exposed to 40.0°C. Relative percent haploids fell below control levels after day 11 with a corresponding rise in the relative percentage of diploid and tetraploid cells. The greatest effect of testicular heat stress was seen in 42.0°C exposed mice. The percent haploids maintained a significant relative decrease ($P < 0.001$) day

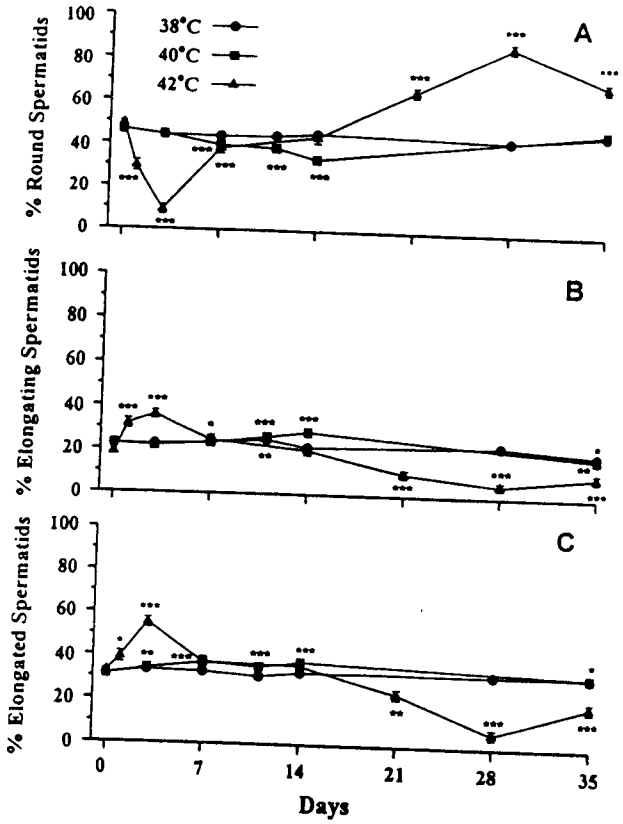

FIG. 4 Effects of scrotal heat on acridine orange-stained mouse testicular round (A), elongating (B), and elongated (C) spermatid populations (LSMeans ± SEM) plotted over time after thermal exposure and calculated from gated regions of computer generated flow cytometric cytograms similar to those in shown in Figure 2B. Control values are plotted as day 0. Percentage round, elongating, and elongated spermatids did not differ between the control group for 38.0°C and 40.0°C exposure and the control group for 42.0°C exposure. * = $P < 0.05$; ** = $P < 0.01$ *** = $P < 0.001$.

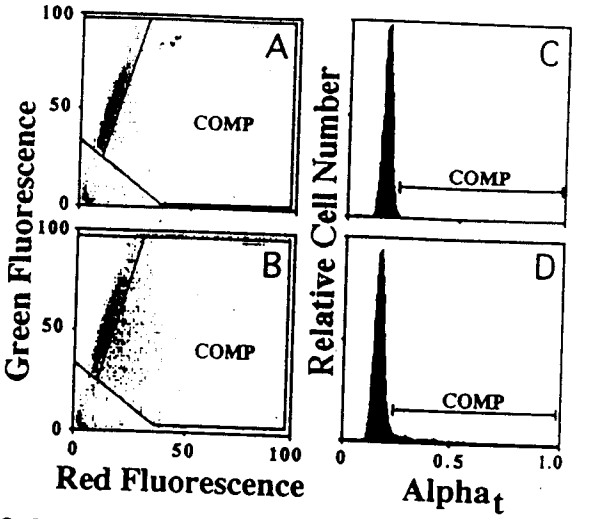

FIG. 5. Flow cytometric green- (dsDNA) vs. red- (ssDNA) fluorescence cytograms (A, B) and α_t histograms (C, D) from SCSA measurements of acid-stressed, acridine orange-stained cauda epididymal sperm from a control mouse (A, C) and from a mouse 11 days after scrotal exposure to 40.0°C (B, C). Both types of plots demonstrate the percentage of cells outside of the main population of α_t (COMPα_t); i.e., the gated areas in plots A and B, and the designated line in C and D. Cellular debris corresponds to the dots near the origin and are gated out as shown in A and B, thus excluding debris from the data analyzed in panels C and D. The theoretical values of α_t range from zero to one; however, for convenience of working with whole numbers, α_t values are expressed in this study (see Fig. 6) as ranging from zero to 1,000.

3 through day 35, resulting in a significant relative increase in the percent of diploid cells (day 1; $P < 0.05$, all others; $P < 0.001$). Relative percent tetraploids differed on all days except day 14.

Changes in relative percentage of the three haploid subpopulations (round, elongating, and elongated spermatids) were also temperature dependent (Fig. 4). The 38.0°C exposure did not affect the percent round or elongated spermatids, and only minor differences were seen in the percent elongating spermatid populations ($P < 0.01$). The relative percentages of all three spermatid populations differed after 40.0°C and 42.0°C exposure ($P < 0.001$). Relative decreases on days 7, 11, and 14 for percent round spermatids at 40.0°C exposure resulted in relative increases in the elongating and elongated spermatid populations. The 42.0°C exposure caused the most changes in haploid populations; significant initial decreases in percent round spermatids on days 1, 3, and 7 and subsequent increases on days 21, 28, and 35 occurred with percent elongating and elongated spermatid populations reflecting those changes.

Caudal Sperm

SCSA data on $X\alpha_t$, $SD\alpha_t$, and $COMP\alpha_t$ were dependent on exposure to temperature and time of recovery (Figs. 5, 6A–C). The caudal epididymides of the 42.0°C group did not have adequate numbers of sperm for SCSA evaluation; thus, only the data from the 38.0°C and 40.0°C groups are shown in Figure 6. The 38.0°C treated mice exhibited SCSA values similar to the controls for most days. The $SD\alpha_t$ values (Fig. 6B) showed the largest difference between controls and 40.0°C treated mice with a significant increase in value by day 11 ($P < 0.001$) and a return to control levels by day 35. $COMP\alpha_t$ (Fig. 6C) showed a dose response that followed the same pattern as seen with $SD\alpha_t$ (day 3: $P < 0.05$; days 7, 11, and 14: $P < 0.001$). Scrotal heat stress at 40.0°C did not cause significant sperm head morphological changes until day 7 ($P < 0.01$; Fig. 6D). On day 14, 40.0°C exposure resulted in 48% of sperm with abnormal head morphology (7 × control), whereas 38.0°C exposure did not cause more than 21% sperm head abnormalities (3 × control) at any sampling time point.

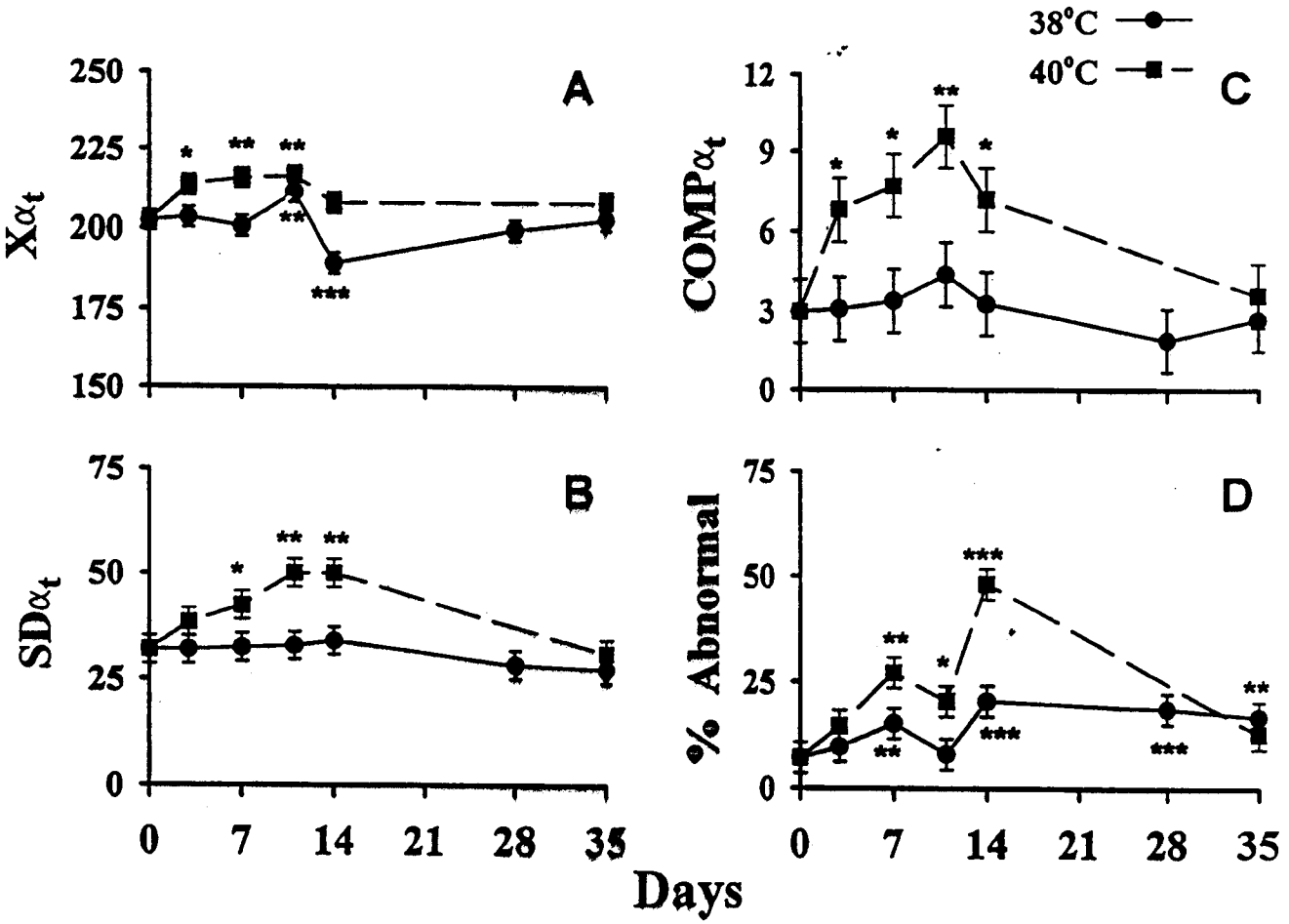

FIG. 6. Graphs of SCSA data (LSMean ± SEM) including $X\alpha_t$ (A), $SD\alpha_t$ (B), and $COMP\alpha_t$ (C) calculated from α_t histograms similar to those in Figure 5. Figure 6D shows the effects (LSMean ± SEM) of scrotal heat on sperm head morphology. A minimum of 1,000 sperm heads per time point were evaluated for head morphology (three mice × 350 sperm heads per mouse). Scrotal regions were exposed to 38.0°C, 40.0°C, or 42.0°C (all ±0.1) for 60 minutes. Control mice were anesthetized without exposure to elevated temperatures. Three mice were thermally exposed for each time point studied for each temperature level. The 38.0°C mice (n = 18) were killed on days 3, 7, 11, 14, 28, and 35, while 40.0°C mice (n = 15) were killed on days 3, 7, 11, 14, and 35. The 42.0° (n = 21) thermally exposed mice did not have adequate numbers of sperm for SCSA evaluation. Controls (n = 9) are plotted as day 0. * = $P < 0.05$; ** = $P < 0.01$; *** = $P < 0.001$.

Discussion

This study has shown altered spermatogenesis resulting from mouse scrota exposure to an elevated temperature (38.0°C to 42.0°C) water bath for 60 minutes. Increased thermal stress in increments of 2.0°C showed very minor disturbances (38.0°C), moderate alterations (40.0°C), and severe disruption of spermatogenesis (42.0°C). Previously, De Vita et al (1990) reported the onset of testicular-weight recovery 28 days after scrotal heat exposure to 42.0°C, while our data spanning 35 days showed a recovery for mice exposed to 40.0°C but not 42.0°C. These decreases in testicular weight are likely due to depletion of hyperthermia-sensitive cells from the testis that was manifest in cauda epididymal samples from mice exposed to 42.0°C.

Differences in spermatogenesis in response to thermal stress were measured in this study by: 1) testicular-weight loss, 2) changes in testicular-cell-type ratios, 3) sperm head morphology, and 4) alterations of caudal sperm chromatin structure, defined as an increased susceptibility to DNA denaturation *in situ*. Acridine orange staining of testicular samples indicated that damage was evident 1 day after exposure to 42.0°C. Significant relative increases in the tetraploid (Fig. 3A) and corresponding decreases in the diploid populations (Fig. 3B) are evidence of a disruption in spermatogenesis, leading to altered ratios of testicular-cell types. Exposure to 42.0°C appears to have affected cells at virtually all stages of spermatogenesis; the effects of 40.0°C were more selective, and 38.0°C showed no measurable alterations of testicular cell populations. Thus, mild hyperthermia exposure did not disrupt spermatogenesis, while higher temperatures had differential effects. Previous reports have indicated that late

spermatocytes are the cell type most susceptible to heat exposure (De Vita et al, 1987, 1990), and our results from mice exposed to 40.0°C concur. Even though the overall relative percentage of haploid testicular cells is unchanged until 11 days after exposure to 40.0°C, the relative percentages of round and elongated spermatids are altered 7 days post heat stress (Fig. 4A and 4C). By utilizing the timetable of spermatogenesis proposed by Oakberg (1956a,b) and Sega (1974), the affected round spermatid population would have been at or prior to the spermatocyte stages at the time of heat stress; interpretations, however, need to take into account the previous observations of Meistrich et al (1973a) that elevated temperatures alter the kinetics of spermatogenesis in mice, essentially increasing the rate of cell differentiation.

Using AO to study testicular populations has the added advantage of resolving the three haploid-cell populations based on RNA content and the degree of chromatin condensation (Fig. 2). De Vita et al (1987, 1990), utilizing only DNA stainability, were only able to distinguish two haploid populations, round and elongating + elongated. Changes in the haploid populations are not as evident when studying only DNA stainability since a change in the elongating population may be masked by a corresponding change in the elongated population thus appearing normal on DNA-staining histograms.

Abnormal sperm chromatin structure was evident 3 days postexposure to 40.0°C (Fig. 6A and 6C). Cauda epididymal sperm at this time point would have been traversing the caput and corpus epididymides during exposure to elevated temperatures. These cells undergo further chromatin condensation including intra- and inter-molecular S–S bonding between protamine cysteine-SH residues (Balhorn et al, 1984). Exposure to thermal stress apparently led to alterations of chromatin packaging measured as an increased sensitivity to DNA denaturation *in situ*.

The SCSA appears to be more sensitive to damage caused by elevated scrotal temperatures (40.0°C) than AO staining of testicular samples or traditional sperm head morphology evaluations. This increased sensitivity of the SCSA vs. other toxicological endpoints has been seen in previous studies, e.g., methyl methanesulfonate (Evenson et al, 1993) and ionizing radiation (Sailer et al, 1995). In this study on thermal exposure, both the $COMP\alpha_t$ and $X\alpha_t$ showed significant increases 3 days following 40.0°C exposure, thus making these variables more sensitive endpoints than sperm head morphology. Along with increased sensitivity, the SCSA also yields more information on the testicular populations affected by increased temperatures. SCSA variables are elevated through day 14 for mice exposed to 40.0°C (Fig. 6), which corresponds to all stages of spermiogenesis or spermatid development (Oakberg, 1956a,b; Sega, 1974). Analysis of sperm with the SCSA as compared to morphology analysis with the light microscope is rapid, objective, and statistically significant (5,000 cells per sample × 3 animals × 2 subsamples = 30,000 cells analyzed vs. 1,000 cells per time point for morphology analysis).

References

Balhorn R, Weston S, Thomas C, Wyrobek AJ. DNA packaging in mouse spermatids: synthesis of protamine variants and four transition proteins. *Exp Cell Res* 1984;150:298–308.

Ballachey BE, Hohenboken WD, Evenson DP. Heterogeneity of sperm nuclear chromatin structure and its relationship to bull fertility. *Biol Reprod* 1987;36:915–925.

Casady RB, Myers RM, Legates JE. The effect of exposure to high ambient temperature on spermatogenesis in the dairy bull. *J Dairy Sci* 1953;36:14.

Chowdhury AK, Steinberger E. A quantitative study of the effect of heat on germinal epithelium of rat testes. *Am J Anat* 1964;115:509–524.

Collins P, Lacey D. Studies on the structure and function of the mammalian testis. II. Cytological and histochemical observations on the testis of the rat after a single exposure to heat applied for different lengths of time. *Proc R Soc Lond Biol Sci* 1969;172:17–38.

Darzynkiewicz Z. Acridine orange as a molecular probe in studies of nucleic acids *in situ*. In: Melamed M, Mullaney P, Mendelsohn M, eds. *Flow Cytometry and Sorting*. New York: John Wiley and Sons; 1979:285–316.

Darzynkiewicz Z, Traganos F, Sharpless T, Melamed MR. Thermal denaturation of DNA *in situ* as studied by acridine orange staining and automated cytofluorometry. *Exp Cell Res* 1975;90:411–428.

Darzynkiewicz Z, Traganos F, Sharpless T, Melamed MR. Lymphocyte stimulation: a rapid multiparameter analysis. *Proc Natl Acad Sci USA* 1976;73:2881–2884.

De Vita R, Calugi A, Chiarantano C, Forte D, Mauro F, Uccelli R. Effects of heat on mouse spermatogenesis monitored by flow cytometry. *Int J Hyperthem* 1990;6:543–551.

De Vita R, Calugi A, Forte D, Chiarantano C, Uccelli R, Vizzone A, Mauro F. Cellular effects of heat on mouse spermatogenesis. In: Burger G, Ploem JS, Goerttler K, eds. *Clinical Cytometry and Histometry*. London: Academic Press; 1987:300–302.

Evenson DP. Flow cytometry evaluation of male germ cells. In: Yen A, ed. *Flow Cytometry Advanced Research and Clinical Applications*. Vol I. Boca Raton, Florida: CRC Press; 1989:217–246

Evenson DP. Flow cytometry assays of male fertility. In: Darzynkiewicz Z, Crissman H, eds. *Methods in Cell Biology*. Vol 33. *Flow Cytometry*. New York: Academic Press; 1990:401–410.

Evenson DP, Baer RK, Jost LK. Long term effects of triethylenemelamine exposure on mouse testis cells and sperm chromatin structure assayed by flow cytometry. *Environ Mol Mutagen* 1989;14:79–89.

Evenson DP, Baer RK, Jost LK, Gesch RW. Toxicity of thiotepa on mouse spermatogenesis as determined by dual-parameter flow cytometry. *Toxicol Appl Pharmacol* 1986a;82:151–163.

Evenson DP, Darzynkiewicz Z, Jost L, Janca F, Ballachey B. Changes in accessibility of DNA to various fluorochromes during spermatogenesis. *Cytometry* 1986b;7:45–53.

Evenson DP, Darzynkiewicz Z, Melamed MR. Relation of mammalian sperm chromatin heterogeneity to fertility. *Science* 1980;210:1131–1133.

Evenson DP, Higgins PH, Grueneburg D, Ballachey BE. Flow cytometric analysis of mouse spermatogenic function following exposure to ethylnitrosourea. *Cytometry* 1985;238–253.

Evenson DP, Jost LK. Hydroxyurea exposure alters mouse testicular kinetics and sperm chromatin structure. *Cell Prolif* 1993;26:147–159.

Evenson DP, Jost LK. Sperm chromatin structure assay: DNA denaturability. In: Darzynkiewicz Z, Robinson JP, Crissman HA, eds. *Flow Cytometry*. 2nd ed. *A Volume of Methods in Cell Biology*. Vol 42. Orlando, Florida: Academic Press; 1994:159–176.

Evenson DP, Jost LK, Baer RK. Effects of methyl methanesulfonate on mouse sperm chromatin structure and testicular cell kinetics. *Environ Mol Mutagen* 1993;21:144–153.

Evenson DP, Jost LK, Baer RK, Turner TW, Schrader SM. Individuality of DNA denaturation patterns in human sperm as measured by the sperm chromatin structure assay. *Rep Toxicol* 1991;5:115–125.

Evenson DP, Melamed MR. Rapid analysis of normal and abnormal cell types in human semen and testis biopsies by flow cytometry. *J Histochem Cytochem* 1983;31:248–253.

Evenson DP, Thompson L, Jost L. Flow cytometric evaluation of boar semen by the sperm chromatin structure assay as related to cryopreservation and fertility. *Theriogenology* 1994;41:637–651.

Hand JW, Walker H, Hornsey S, Field SB. Effects of hyperthermia on the mouse testis and its response to X-rays, as assayed by weight loss. *Int J Radiat Biol* 1979;6:521–528.

Levine RJ, Mathew RM, Chenault CB, Brown MH, Hurtt ME, Bentley KS, Mohr KL, Working PK. Differences in the quality of semen in outdoor workers during summer and winter. *New Engl J Med* 1990;323:12–16.

Meistrich ML, Brock WA, Grimes SR, Platz RD, Hnilica LS. Nuclear protein transitions during spermatogenesis. *Fed Proc* 1978;37:2522–2525.

Meistrich ML, Bruce WR, Clermont Y. Cellular composition of fractions of mouse testis cells following velocity sedimentation separation. *Exp Cell Res* 1973a;79:213–227.

Meistrich ML, Eng VWS, Loir M. Temperature effects on the kinetics of spermatogenesis in the mouse. *Cell Tiss Kinet* 1973b;6:379–393.

Mieusset R, Casares Q, Sanchez-Partida LG, Sowerbutts SF, Zupp JL, Setchel BP. The effects of moderate heating of the testes and epididymides of rams by scrotal insulation on body temperature, respiratory rate, spermatozoa output and motility, and on fertility and embryonic survival in ewes inseminated with frozen semen. In: Robaires B, ed. The male germ cell: spermatogonium to fertilization. *Ann NY Acad Sci* 1991;637:445–457.

Monesi V. Synthetic activities during spermatogenesis in the mouse: RNA and protein. *Exp Cell Res* 1965;39:197–224.

Oakberg EF. Sensitivity and time of degeneration of spermatogenic c. irradiated in various stages of maturation in the mouse. *Rad Res* 1955;2:369–391.

Oakberg EF. A description of spermiogenesis in the mouse and its use in analysis of the cycle of the seminiferous epithelium and germ cell renewal. *Am J Anat* 1956a;99:391–413.

Oakberg EF. Duration of spermatogenesis in the mouse and timing of stages of the cycle of the seminiferous epithelium. *Am J Anat* 1956b; 99:507–516.

Russell LD, Ettlin RA, Sinha Hikim AP, Clegg ED, eds. *Histological and Histopathological Evaluation of the Testis*. Clearwater, Florida: Cache River Press; 1990.

Sailer BL, Jost LK, Erickson KR, Tajiran MA, Evenson DP. Effects of x-irradiation on mouse testicular cells and sperm chromatin structure. *Environ Mol Mutagen* 1995;25:23–30.

Sega GA. Unscheduled DNA synthesis in the germ cells of male mice exposed *in vivo* to the chemical mutagen ethyl methanesulfonate. *Proc Natl Acad Sci USA* 1974;71:4955–4959.

Sega GA, Owens JG. Methylation of DNA and protamine by methyl methanesulfonate in the germ cells of male mice. *Mutation Res* 1983;111:227–244.

The Statistical Analysis System for Windows. Release 6.11. Cary, North Carolina: Statistical Analysis Systems Institute, Inc; 1996.

Ulberg LC. The influence of high temperature on reproduction. *J Hered* 1958;49:62–64.

Vogler CJ, Saacke RG, Bame JH, DeJarnette JM, McGilliard ML. Effects of scrotal insulation on viability characteristics of cryopreserved bovine semen. *J Dairy Sci* 1991;74:3827–3835.

Westra A, Dewey WC. Variation in sensitivity to heat shock during the cell-cycle of Chinese hamster cells *in vitro*. *Int J Radiat Biol Relat Stud Phys Chem Med* 1971;19:467–477.

Wyrobek AJ, Bruce WR. Chemical induction of sperm abnormalities in mice. *Proc Natl Acad Sci USA* 1975;72:4425–4429.